TURBULENT RAMP FLOW CONTROL BY MEANS OF A PERTURBATION DOWNSTREAM OF FLOW SEPARATION

Nicolas Mazellier
Flows and Aerodynamic Systems Department
University of Orleans, INSA-CVL, PRISME, EA 4229
F45072, Orleans, France
nicolas.mazellier@univ-orleans.fr

Pierric Joseph
Flows and Aerodynamic Systems Department
University of Orleans, INSA-CVL, PRISME, EA 4229
F45072, Orleans, France
pierric.joseph@univ-orleans.fr

Francesco Stella
Flows and Aerodynamic Systems Department
University of Orleans, INSA-CVL, PRISME, EA 4229
F45072, Orleans, France
franscesco.stella@etu.univ-orleans.fr

Azeddine Kourta
Flows and Aerodynamic Systems Department
University of Orleans, INSA-CVL, PRISME, EA 4229
F45072, Orleans, France
azeddine.kourta@univ-orleans.fr

Patricia Sujar-Garrido
Institute for Turbulence-Noise-Vibration
Interaction and Control
Shenzhen Graduate School
Harbin Institute of Technology
Xili University Town, Shenzhen, 518055, China
patricia.sujar@gmail.com

Yu Zhou
Institute for Turbulence-Noise-Vibration
Interaction and Control
Shenzhen Graduate School
Harbin Institute of Technology
Xili University Town, Shenzhen, 518055, China
yuzhou@hit.edu.cn

ABSTRACT

We report an experimental investigation of the control of the separated turbulent flow on a backward-facing ramp. The actuation is performed by means of a 2D synthetic jet located slightly downstream of upper edge of the ramp. It is shown that at the best operating condition of the actuator, separation almost collapses. Phase-averaged velocity fields are investigated to get some insights about the mechanisms at play during control. Our analysis suggests that the vortex pair issuing from the synthetic jet undergoes a precession motion inducing the separation mitigation. A simple mechanism is proposed and discussed to account for the early stage of interaction between the separated flow and the actuation.

INTRODUCTION

Separating/reattaching flows are of primary importance in a number of industrial applications, encompassing bluff bodies such as ground vehicles, streamlined bodies such as wings and blades at high incidence/pitch angle, combustion chambers, turbines and pipelines. In most of these applications, flow separation leads to detrimental effects such as losses of aerodynamic performances (drag increase, lift decrease or both) or intense unsteady structural loads eventually leading to accelerated structural fatigue. This means that flow separation avoids the use of these systems at their nominal operating conditions. To mitigate its effects, over the past decades great attention has been paid to prediction of flow separation and its control (see e.g. McCormick, 2000; Darabi & Wygnanski, 2004; Dandois et al., 2007; Debien et al., 2016 among others). A key point underlying control design relates to the detailed knowledge of the interaction between the separated flow and the actuator. This study aims at addressing this issue by combining and comparing results obtained in two experimental facilities (University of Orléans, Harbin Institute of Technology) using two control strategies (synthetic jets vs. pulsed jets). The objectives pursued within this joint work are twofold: i. assessing control strategy performances and ii. getting a better understanding of the mechanisms driving the interaction between the separation and the actuation. It is worth noting that since two different actuation techniques are used, we expect control mechanisms to be different.

To achieve these goals, the flow over a descending ramp is used as a prototype of separating/reattaching flow. Within this paper, we present the first outcomes of this cooperative work by focusing on the results obtained at the University of Orléans, which were dedicated to the effect of synthetic jets set downstream the separation. The paper is organized as follows: the experimental set-up is described first. Then, the main results are presented and finally discussed through a possible interaction mechanism.

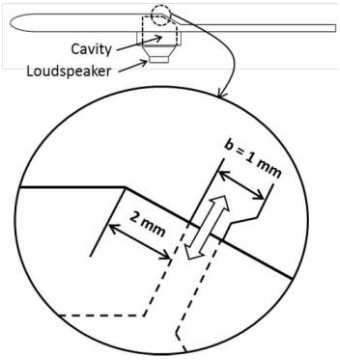

Figure 1. Schematic of the ramp model and actuators. The incoming flow goes from left to right.

EXPERIMENTAL SET-UP

Results reported in this paper have been obtained at the University of Orléans in a closed-loop wind tunnel with a 5 m long

and 2×2 m^2 test section. More details about the experimental facility can be found in Kourta et al. (2015). A schematic of the ramp model is displayed in Fig. 1 together with the implementation of the control actuators. The ramp is 100 mm high with a constant slope of 25°. The model is set at the mid-height of the wind-tunnel and spans its entire width. This set-up allows a nearly zero-pressure gradient turbulent boundary layer to develop up to the leading edge of the ramp. The incoming boundary-layer is tripped and so is turbulent. For sake of simplicity, we report only results obtained for $Re_\theta = U_0\theta/\nu \approx 3000$ (with U_0 the free-stream velocity, θ the momentum thickness of the boundary layer and ν the kinematic viscosity).

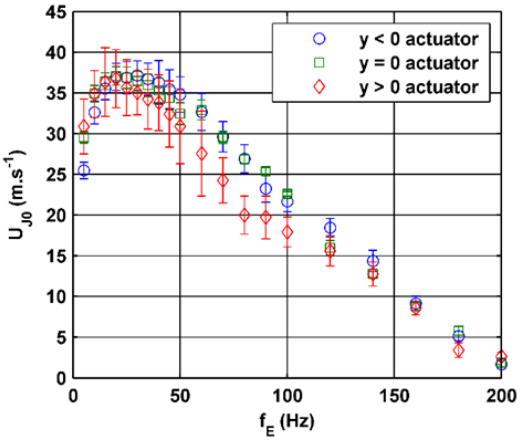

Figure 2: typical maximum exhaust velocity measured by means of hot-wire (blowing phase only) as a function of excitation frequency. Error bars represent the standard deviation (± 2σ) of the measured peak velocities.

In this paper, flow control is achieved by means of synthetic jets (Smith & Glezer, 1998) generated by three loudspeakers located underneath the model upper slant edge (see Fig. 1). The inner cavities and the external flow are connected via a bi-dimensional slot (1 mm wide) spanning the entire width of the model. The slot is located 2 mm downstream of the upper edge of the ramp. These actuators can run within a wide range of operating conditions which are characterized by the dimensionless frequency $F^+ = f_E h/U_0$ and the momentum coefficient $C_\mu = bU_{j0}^2/(hU_0^2)$ with f_E the actuation frequency, h the ramp height, b the slot width and U_{j0} the maximum jet exhaust velocity (see Fig. 2). An extensive parametric study has been carried out by varying independently these two control parameters. In the following, we report only results obtained for the best open-loop control case ($F^+ = 0.2$, $C_\mu = 0.04$), which leads to the smallest mean recirculation bubble. These operating conditions coincide to the plateau of exhaust velocity at low actuation frequency ($f_E \approx 40\ Hz$) as evidenced in Fig. 2. Note that at this frequency, the 3 actuators behave similarly. Mean velocity fields as well as fluctuating velocity components were investigated by means of Particles Image Velocimetry (PIV). Measurements are focused on an area surrounding the ramp (see Fig. 3). Laser light is provided by a 200 mJ / 15 Hz / 532 nm Quantel Evergreen 200-10 Nd:YAG laser illuminating olive oil particles used to seed the flow. Illuminated images are recorded by means of two cameras LaVision Imager LX 11M with a resolution of 4032 × 2688 pixels. Taking into account the overlap between the fields of view (FOV) of each camera, the investigated area is 628 mm long (x direction) and 319 mm high (z direction). A multi-pass process is used with an initial interrogation window of 64×64 pixels and a second one of 32×32 pixels. Considering the final size of the interrogation window and a 50% overlap, a spatial resolution of 1.89 mm is achieved in both x and z directions. Note also that free-stream velocity U_0 and ramp height h are used as scaling parameters, in the following.

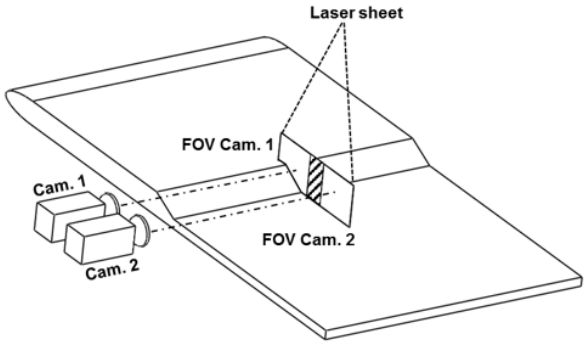

Figure 3: Schematic of PIV set - up.

1-POINT STATISTICS

In the following, we discuss the main features of the 1-point statistics. To this end, Reynolds decomposition is deployed, i.e. the velocity u is decomposed into a mean (U) and a fluctuating (u') components. The mean flow computed from the PIV data in both uncontrolled and controlled cases is shown in Fig. 4. As expected, the baseline configuration is characterized by a massive separation onsetting at the upper edge of the ramp. The length of the resulting mean recirculation bubble is comparable to that reported in Kourta et al. (2015). The best open-loop control case is characterized by an impressive reduction of the recirculation bubble (≈ 75% reduction), emphasizing the control efficiency.

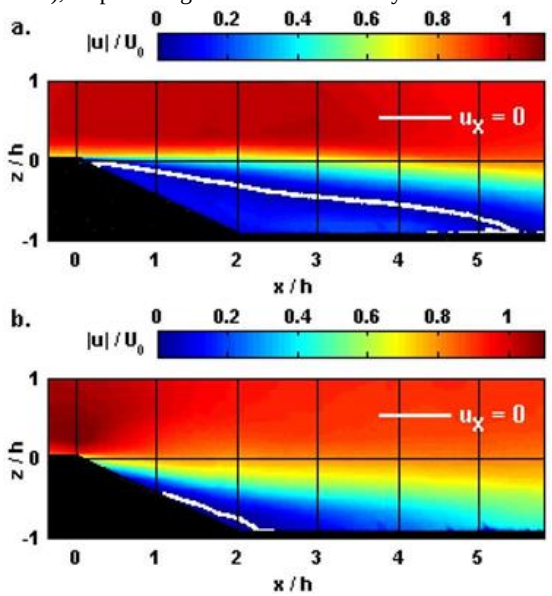

Figure 4: Dimensionless mean streamwise velocity computed from PIV for (a) uncontrolled and (b) open-loop controlled cases. The white line stands for the mean separation location.

The turbulent kinetic energy (at least its surrogate accessible by 2D-2C PIV) $k = \frac{1}{2}(\langle u'^2 \rangle + 2\langle v'^2 \rangle)$ (with $\langle u'^2 \rangle$ and $\langle v'^2 \rangle$ the normal Reynolds stresses in the streamwise and wall normal directions, respectively) is displayed in Fig. 5 for both uncontrolled and controlled cases. Combining the effects of the mixing layer onsetting at the separation point and the flapping of recirculation bubble, k increases all along the separation until reaching its maximum value close to the reattachment point for the uncontrolled case. This is well supported by the production term, P, which is mainly concentrated in the separated shear layer. Differently from the uncontrolled case, the production is predominant in the vicinity of the upper edge of the ramp (see Fig. 6). This leads to high values of k close to the separation point and then it decays and spreads (see Fig. 5). The turbulent kinetic energy increases with the control and expands on large transversal zone compared to the uncontrolled case.

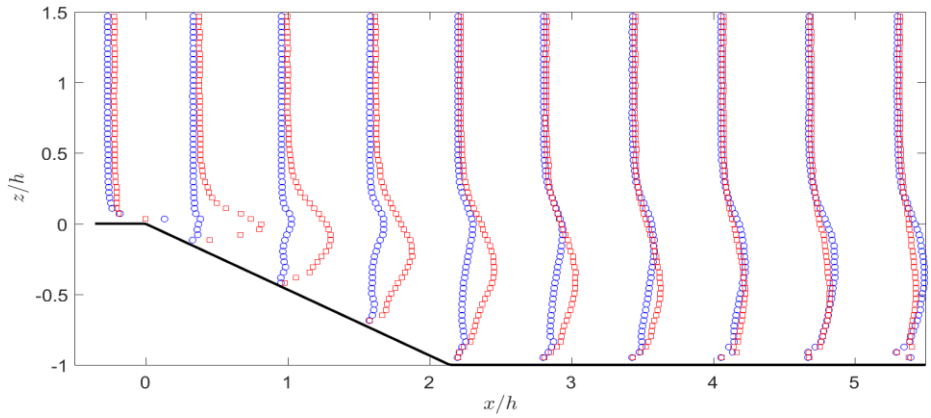

Figure 5. Turbulent kinetic energy profiles over the ramp for the uncontrolled (blue circles) and the controlled (red squares).

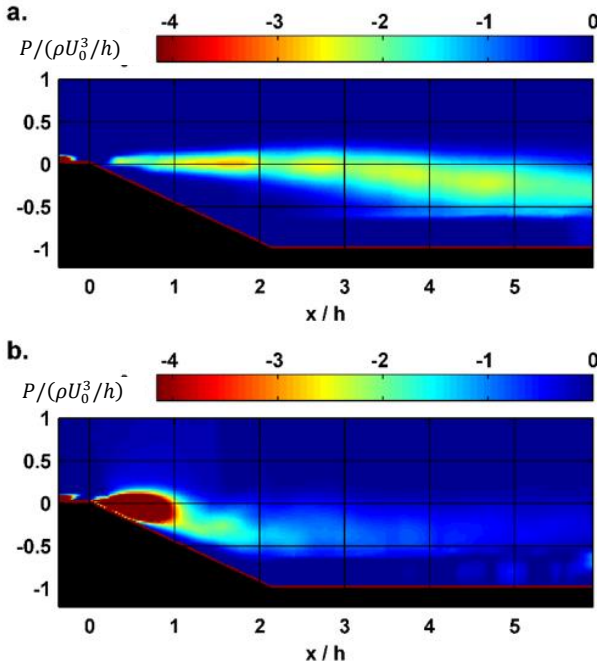

Figure 6: dimensionless production of turbulent kinetic energy for the uncontrolled (a) and controlled (b) cases.

To assess the control efficiency in average, a mean energy budget has been performed over the control volume represented in Fig. 7. To that purpose, the terms of the mean energy transport equation have been inferred from PIV measurements. The pressure terms being calculated from the mean momentum transport equations (van Oudheusden et al, 2007). From this approach, it is found that the head losses induced by the abrupt geometrical expansion is reduced by around 23% when control is applied. Our results show that the production of turbulent kinetic energy and the work of the turbulent stresses are the main contributors to the head losses. Furthermore, the production terms are almost equivalent in magnitude, albeit the mechanisms underlying the uncontrolled and controlled flows are different. This means that the control essentially modifies the work of the Reynolds stresses.

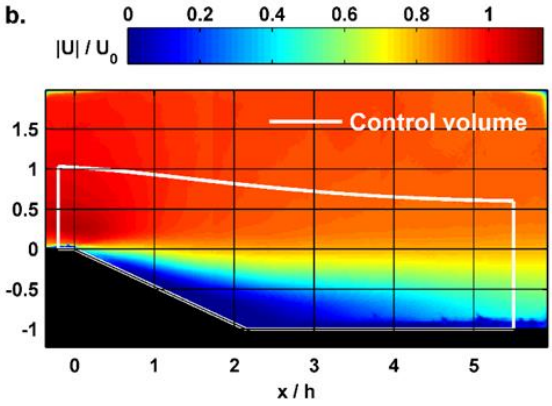

Figure 7: typical control volume used to perform the mean energy budget. The upper edge is a streamline.

DYNAMICS OF THE CONTROL

To get a better understanding of the physical mechanisms underlying the interaction between the flow and the actuation, the dynamics of the controlled flow has been investigated by means of triple decomposition ($u = U + \tilde{u} + u'$ with $\tilde{u}$ the coherent fluctuation) to discriminate between organized and turbulent motions.

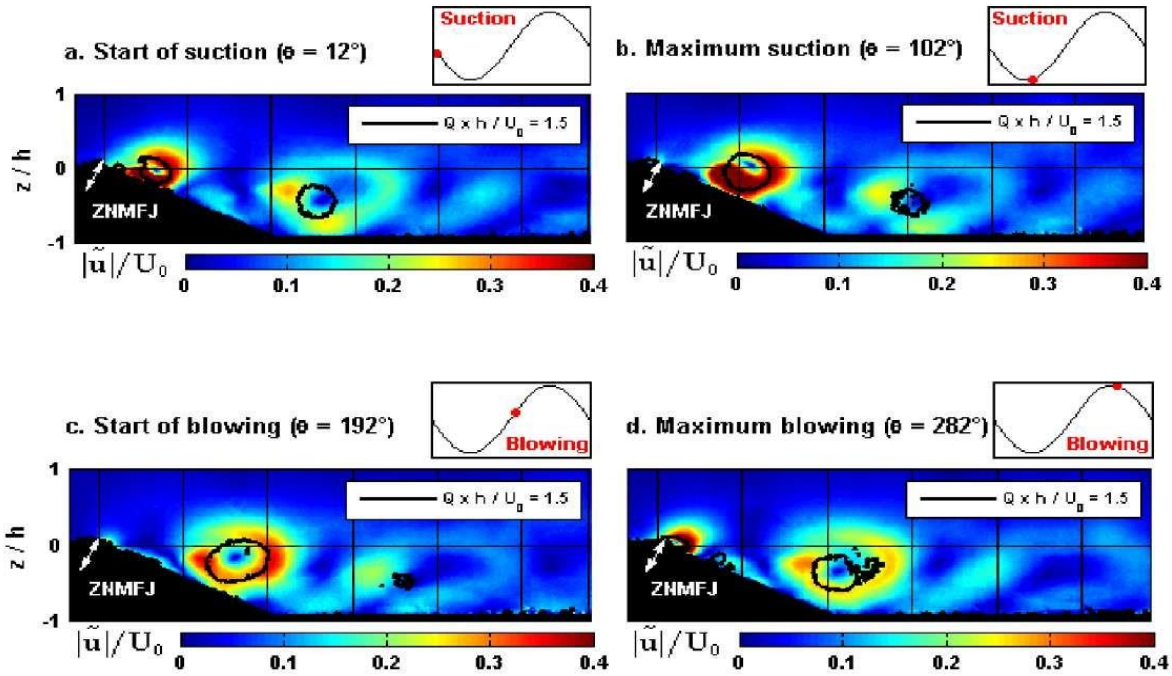

Figure 8. Dimensionless phased-averaged streamwise velocity. The inserts indicate the phase. The black lines stand for the contour of the Q-criterion. The white arrows indicate the location of the slot.

For that purpose, PIV data have been gathered together with the electric signal used to supply the loudspeakers. Then, data have been phase-averaged using the supplying voltage as phase reference. The phase-averaged streamwise velocity computed at phases φ = 12°,102°,192° and 282° are displayed in Fig. 8 which emphasizes the formation of a vortex pair issuing from the synthetic jet during the blowing phase. Then these vortices are convected along the ramp in a downward motion. These vortices induce convection of momentum from high momentum potential flow toward the wall, which leads to the recirculation bubble reduction. Since these coherent structures are mostly intense up to the foot of the ramp meaning that they account for the large production concentrated in the vicinity of the upper edge of the ramp (see Fig. 6) and therefore contribute to the high values of turbulent kinetic energy observed in Fig. 5.

During this motion, our data suggest that a precession of the vortex pair occurs. This mechanism is depicted in Fig. 9 at the early stage of the interaction between the separated flow and the actuator. In this proposed scenario, the vortex pair resulting from the blowing phase is first convected along the synthetic jet axis since the flow is almost at rest in that region. Then the upstream vortex penetrates through the separation line where its trajectory is modified by the local velocity (eventually changing its rotation direction) breaking the symmetry of the vortex pair. During the suction phase, the downstream vortex is convected upward to the wall increasing thereby its circulation. This causes the separation line to move toward the wall reducing thereby the recirculation area. Note that this scenario may also apply when separation collapses. While moving further downstream, the vortex pair diffuses (see phase φ= 192° in Fig. 8) and then deviates slightly

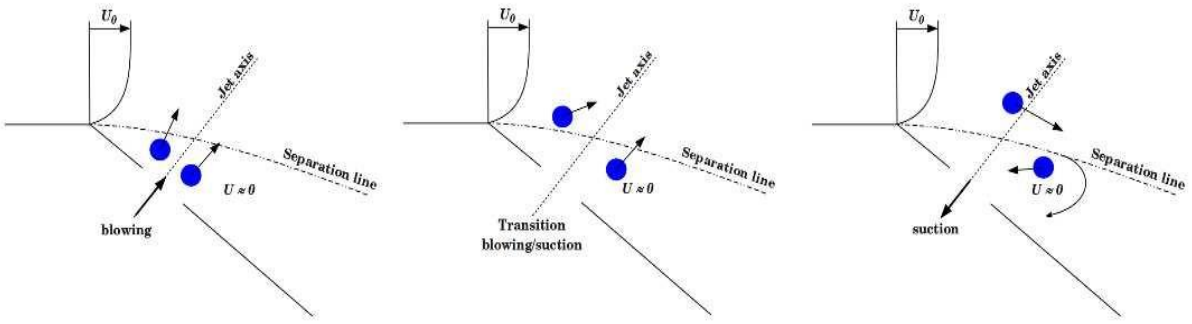

Figure 9. Schematic of the flow/actuator interaction at the early stage of control.

from the wall due to the local adverse pressure gradient leading to a restricted separation (see Fig. 4). Note that a case using a larger C_μ has enabled to fully collapse the recirculation bubble probably by enhancing the vortex pair circulation.

CONCLUSIONS

In this work, a turbulent separated flow over a backward-facing ramp has been controlled with synthetic jets by varying the control operating conditions. Reported results in this study have been obtained with an actuation located downstream of the ramp upper edge. As emphasized by the 1-point statistics analysis, the mean separation almost collapses (≈ 75% reduction) for the best open-loop case. However, the cost to be paid ($C\mu$ = 0.04) for such impressive reduction is large. The main change is the production of high fluctuating energy close to the separation point which leads to a reduction of the work of the Reynolds stresses. In average, a decrease by 23% of the head losses has been observed. Phase-averaged analysis has evidenced that the actuation produces organized structures that break the recirculation bubble, causing the reduced reattachment length. A first simple mechanism of flow/actuator interaction has been proposed to account for their precession motion. Further studies are currently in progress to assess this interaction. We also aim at extending this study by setting the actuation location upstream from the ramp leading edge to compare with the work performed at HIT using the same data analysis (momentum budget, modal decomposition ...) to gain a better understanding of the difference between control mechanisms.

We also observe that the best separation reduction does not correspond to the higher drag reduction case. This has been compared in one submitted paper.

We also deeply analyze the uncontrolled case by focusing in the non-turbulent/turbulent interface in the shear layer at the upper part of the separation. The Recirculation interface was analyzed for the same goal. Global balance of the momentum and energy are established and the important mechanisms are characterized. These results constitute a paper under revision.

Some of these results will be presented in the symposium.

REFERENCES

Dandois, J., Garnier, E. & Sagaut, P. 2007 Numerical simulation of active separation control by a synthetic jet. Journal of Fluid Mechanics 574, 25–58.

Darabi, A. & Wygnanski, I. 2004 Active management of naturally separated flow over a solid surface. part 1. the forced reattachment process. Journal of Fluid Mechanics 510, 105–129.

Debien, A., von Krbek, K., Mazellier, N., Duriez, T., Cordier, L., Noack, B.R., Abel, M.W. & Kourta, A. 2016 Closed-loop separation control over a sharp edge ramp using genetic programming. Experiments in Fluids 57, 1–19.

Kourta, A., Thacker, A. & Joussot, R. 2015 Analysis and characterization of ramp flow separation. Experiments in Fluids 56, 104–119.

McCormick, D.C. 2000 Boundary layer separation control with directed synthetic jets. AIAA paper 519, 2000.

Smith, B.L. & Glezer, A. 1998 The formation and evolution of synthetic jets. Physics of Fluids 10, 2281–2297.

van Oudheusden, B. W., Scarano, F., Roosenboom, E. W., Casimiri, E. W., & Souverein, L. J. 2007. Evaluation of integral forces and pressure fields from planar velocimetry data for incompressible and compressible flows. Experiments in Fluids, 43(2-3), 153-162.